THE JOURNAL OF PHYSICAL CHEMISTRY B

Article

pubs.acs.org/JPCB

Role of the Electrostatic Interactions in the Stabilization of Ionic Liquid Crystals: Insights from Coarse-Grained MD Simulations of an Imidazolium Model

Giacomo Saielli*,† and Yanting Wang‡,§

†CNR Institute on Membrane Technology, Unit of Padova and Department of Chemical Sciences, University of Padova, Via Marzolo, 1-35131 Padova, Italy

‡CAS Key Laboratory of Theoretical Physics, Institute of Theoretical Physics, Chinese Academy of Sciences, 55 East Zhongguancun Road, P.O. Box 2735, Beijing, 100190, China

§School of Physical Sciences, University of Chinese Academy of Sciences, 19A Yuquan Road, Beijing 100049, China

ABSTRACT: In order to investigate the role of the electrostatic interactions in stabilizing various phases of ionic liquids, especially smectic ionic liquid crystals, we have employed a coarse-grained model of 1-hexadecyl-3-methylimidazolium nitrate, $[C_{16}mim][NO_3]$, to perform molecular dynamics simulations with the partial charges artificially rescaled by a factor from 0.7 to 1.2. The simulated systems have been characterized by means of orientational and translational order parameters and by distribution functions. We have found that increasing the total charge of the ions strongly stabilizes the ionic smectic phase by shifting the clearing point (melting into the isotropic liquid phase) to higher temperatures, while a smaller effect is observed on the stability of the crystal phase. Our results highlight the importance of the electrostatic interactions in promoting the formation of ionic liquid crystals through microphase segregation. Moreover, as the total charge of the model is increased, we observe a transformation from a homogeneous to a nanosegregated isotropic structure typical of ionic liquids. Therefore, a connection can be established between the degree of nanosegregation of ILs and the stability of ILC phases. All the above can be understood by the competition among electrostatic interactions between charged groups (cationic head groups and anions), van der Waals interactions between nonpolar cationic tail groups, and thermal fluctuations.

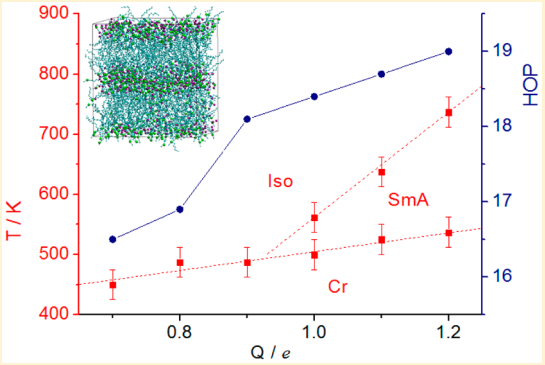

1. INTRODUCTION

Ionic liquid crystals (ILCs) are thermotropic liquid crystals (LC) materials formed by the same kind of organic cations and inorganic anions as typically found in ionic liquids (ILs). ILs are usually composed of quaternized nitrogen cations, such as imidazolium, pyridinium, guanidinium, pyrrolidinium, and inorganic anions such as halides, PF_6^-, BF_4^-, $(CF_3SO_2)_2N^-$.[1−3] When one or more alkyl chains are sufficiently long, the isotropic liquid undergoes one or more transitions into a mesophase before crystallization, thus forming ILCs. The subject has been thoroughly reviewed in the very recent publication of Goossens et al.[4] which covers the last 10 years while a comprehensive account of the previous literature can be found in the 2005 review of Binnemans.[1]

Microphase segregation between the ionic parts and the long alkyl chains is responsible for the formation of smectic (that is layered) mesophases. For imidazolium salts, a smetic A (SmA) phase is observed for chains of at least 12 carbon atoms;[5,6] similarly, silver alkanoates exhibit several smectic phases for chains longer than ten carbon atoms.[7] Viologen dimers have been found to exhibit a SmA phase for lateral chains of 12 carbon atoms or more.[8]

Applications of ILCs in the field of nonlinear optics have been recently reviewed.[9] Other interesting examples of ILC applications concern solar cells,[10,11] membranes for water desalination,[12] battery materials,[13] electrochemical sensors,[14,15] and electrofluorescence switches.[16,17] A more recent example concerning ILCs confined in porous membranes can be found in ref 18. In all these cases, the ordered nature of ILCs is the key property behind the improved performance compared to isotropic ILs, often at the cost, however, of an increased viscosity. It is, therefore, of fundamental importance to investigate the many factors that contribute to the stabilization of ionic mesophases and their properties.

Molecular dynamics (MD) simulations based on fully atomistic (FA) force fields (FF) are a very efficient tool to study the structural and dynamic properties of ILs[19−28] and ILCs[29,30] in a well-defined phase (e.g., the isotropic phase of ILs and the smectic phase for ILCs). FA simulations have also been successfully used to investigate liquid crystals (LCs) in a

Received: May 10, 2016
Revised: August 3, 2016
Published: August 3, 2016

DOI: 10.1021/acs.jpcb.6b04717
J. Phys. Chem. B 2016, 120, 9152−9160

wide temperature and phase range,[31−33] and continuing efforts are devoted to the development of improved FAFF for LCs.[34] However, ILCs usually have a rather large viscosity, since they combine the long-range order of LCs with the strong intermolecular interactions of ILs, and the simulation of their properties is better accomplished using coarse-grained (CG) models, especially if several phases and a wide temperature range are considered.

CG models largely simplify the molecular structure while keeping the essential ingredients (molecular topology, flexibility, and charge distribution) that are responsible for the structural and dynamic properties of the ionic fluid. Although specific interactions are not explicitly included in the CG model, such as hydrogen bonds, these are not essential in determining the phase sequence (crystal-smectic-isotropic) since the same phase behavior is observed with a large variety of salts, as mentioned above, encompassing different kinds of cations and anions. This is further justified by the fact that CG MD simulations were successful in reproducing different phases: in fact, insights on the properties of the ionic smectic phase of a representative compound, $[C_{16}mim][NO_3]$, have been recently reported using MD simulations with a coarse-grained force field (CGFF).[35,36] We have also investigated the effect of varying the alkyl chain length in the homologous series of $[C_nmim][NO_3]$[37] and what are the microscopic structural changes that accompany the transition from the locally nanosegregated isotropic phase into the layered smectic phase.[38] In these two latter papers the role of the van der Waals (VDW) interactions in stabilizing the layered ionic smectic phase was investigated in detail.

On the other hand, in the isotropic phase of ionic liquids the nanosegregation between charged and hydrophobic domains has been first predicted by computer simulations[39−41] then confirmed experimentally.[42] The role of electrostatic interaction in creating a continuum polar network that favors the nanosegregation of the hydrophobic chains has also been clearly highlighted.[43] Moreover, by increasing the temperature, an additional liquid−liquid phase transition, from the nanosegregated structure to a uniform structure was observed by computer simulations.[44]

It is, however, not obvious which should be the best charge to set for a classical description of ionic fluid systems, either ILs or ILCs, when using fully atomistic FFs. The apparently obvious choice of constraining the total charge of cations and anions to integer values may be questioned for several reasons. On one hand, polarizability effects reduce the effective charge on the ions since induced dipoles (and higher multipoles) counteract the electrostatic field from which they stem; thus a simple way to introduce the effect of polarizability in classical MD simulations is to use reduced charges, scaled by a factor around 0.8.[45] On the other hand, it has been found that charge transfer may occur in IL pairs so that the real average charge of the ions in an ionic fluid may be less than unity;[46] in fact, the use of reduced charges to mimic the effect of polarizability and charge-transfer provides diffusion coefficients in better agreement with experiments.[47]

Together with the physically based reasons for investigating ionic systems with a reduced or scaled total charge, it is also of interest, from a purely theoretical viewpoint, to study systems with a larger charge compared to the ±1 values typical of imidazolium salts. There are examples of dicationic systems (therefore with +2 charge) where the two charges are localized on a relatively small moiety of the molecule such as the DABCO derivatives investigated by Nogami and co-workers.[48,49] Similarly, bistriflimide salts of nonsymmetric viologens are another example of dicationic systems with the two charges on the same unit exhibiting a rich polymorphism with an ordered SmX phase[50,51] and, for dimers, a SmA phase.[8,52,53] Examples can also be found concerning ionic liquids with compact dianionic counterions, such as the *closo*-$B_{12}Cl_{12}$ dianion[54] or zinc tetrahalide complexes.[55] Moreover, from the thermodynamic point of view, different IL and ILC phases result from the competition between the electrostatic interactions between charged groups (cationic head groups and anions) and from the VDW interactions between nonpolar cationic tail groups at a finite temperature. Therefore, artificially tuning the charge unit from less than 1 to more than 1 allows one to conveniently study how varying the relative weights of the two kinds of interactions leads to different phases. This is important for understanding the thermodynamics of ILs and ILCs and paves the road for further systematic studies of their phase transitions.

The influence of charges on the stabilization of ionic mesophases was also recently reviewed by Goossens et al. in ref 4. Some experimental observations concerning such effect are the ones by Deschenaux et al. reporting a neutral ferrocene system that was not mesomorphic while the ferrocenium tosylate analogue exhibited a SmA phase;[56] Jankowiak et al. investigated isosteric ionic and nonionic systems and observed a stronger mesomorphism for the ionic ones;[57] Piechocki et al. found qualitatively similar results of larger thermal range of stability of the mesophase in a charged lanthanide derivative compared to its reduced neutral form.[58]

In contrast to real systems, where charges are fixed to formally integer values, computer simulation models offer the invaluable opportunity to scale the charges continuously in order to highlight and isolate the contribution of the magnitude of the charge itself to the stabilization of ionic smectic phases. Therefore, in this work we have used the CGFF model developed by Voth and Wang for the isotropic phase of short-chain imidazolium salts[59,60] and successfully applied by us also to ionic mesophases, as mentioned above, to build several models that differ only in the total charge of the cation and anion, from a minimum of 0.7 to a maximum of 1.2 times the original +1 charge.

2. COMPUTATIONAL DETAILS

The basic ingredients of the CGFF model system have been described in refs 59 and 60. Briefly, one ion pair of 1-hexadecyl-3-methylimidazolium nitrate, $[C_{16}mim][NO_3]$, is composed of 65 atoms. The CGFF reduces the number of particles to 19 by replacing each methyl and methylene unit, the imidazolium ring, and the anion with single interaction sites (see Figure 1). These are the imidazolium ring (A); the methyl group on nitrogen 3 (B); the methylene group on nitrogen 1 (M1) and the next three methylene groups (M2, M3, M4) of the alkyl chain; the remaining 11 methylene groups of the chain (C); the methyl group C16 (E); and the anion (D). Partial charge values for each site are listed in Table 1. All the partial charges on the CG sites have been rescaled by a factor of 0.7, 0.8, 0.9, 1.0 (the original model), 1.1, or 1.2. For each system, labeled as **Q0.7**, **Q0.8**, **Q0.9**, **Q1.0**, **Q1.1**, and **Q1.2**, respectively, the charge of the anion has been rescaled accordingly in order to have a neutral ion pair.

Simulations of 512 CG ion pairs were run in the *NPT* ensemble, using isotropic box fluctuations, with the software

DOI: 10.1021/acs.jpcb.6b04717
J. Phys. Chem. B 2016, 120, 9152−9160

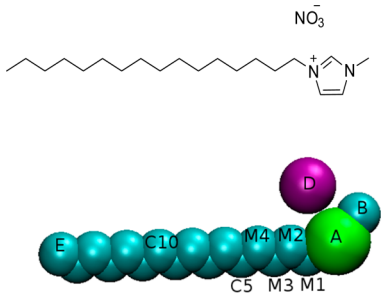

Figure 1. (Top) structural formula and (bottom) coarse-grained model of 1-hexadecyl-3-methylimidazolium nitrate with site labeling.[59,60]

DL_POLY Classic.[61] The size of the system allows the formation of two bilayers in the crystal and SmA phases (within each layer molecules can be arranged with their imidazolium head pointing either up or down). Simulations were run as follows, similarly to the protocol already described in refs 35, 36, and 38. For each model system, we started from the crystal structure at 375 K and we equilibrated the system for several nanoseconds, up to 100−300 ns depending on the system (see Table 2). The configuration obtained after 50 ns at 375 K was used to start another run at 400 K, which also lasted for several nanoseconds. Again the configuration obtained after 50 ns at 400 K was used to start the run at 425 K and so on, with a temperature step of 25 K, until we reached the isotropic phase and the heating sequence of that system was stopped. For the analysis of average properties we have saved the last 25 ns of simulation, at each temperature, every 25 ps for a total of 1000 configurations.

3. RESULTS AND DISCUSSION

3.1. Phase Behavior. We briefly recall here the phase behavior of the model system with a total charge of 1.0 (**Q1.0**). This has been thoroughly investigated in refs 35 and 36 as a model of $[C_{16}mim][NO_3]$. It exhibits three phases: a crystal phase, up to ca. 500 K; a bilayered smectic A phase, between ca. 500 K and ca. 560 K; and an isotropic phase for temperatures higher than 560 K. For this system (total charge 1.0, **Q1.0**) the stability of the three phases was also checked by running, after the first heating sequence, selected cooling runs to confirm the presence of the SmA and crystal (Cr) phases starting from an isotropic and SmA phase, respectively. For the other systems studied here, we only consider the results of the heating runs. It should be noted that the transition temperatures of the model system are not in agreement with the real transition temperatures of $[C_{16}mim][NO_3]$. This has been discussed in ref 35 and 36 and can be related to the fact that the FF has been coarse-grained for the isotropic liquid phase of ILs rather than for the smectic phase of ILCs. Therefore, a quantitative agreement cannot be expected. Nevertheless, using the model system as a tool to modulate the electrostatic interaction, as we do here, will provide valuable insights on the phase behavior.

The identification of the phases (either crystal, smectic or isotropic) was performed by calculating three main properties which quantitatively reveals the structural details of a system: (*i*) the density profile $\rho(z)$ along the director (here the z axis) of a given molecular site, which is expected to be highly modulated for the ordered crystal phase; modulated, though with less features, for the layered smectic phase; and constant for the isotropic phase (it would also be constant for the case of a nematic phase, which is very rarely encountered in ionic systems). (*ii*) the orientational and (*iii*) the translational order parameters, $\langle P_2(\cos\beta)\rangle$ and $\langle\tau\rangle$, respectively. These latter properties will be described in more details in the following. Qualitatively, an isotropic phase is characterized by $\langle P_2\rangle = 0$ and $\langle\tau\rangle = 0$, while for a smectic phase both $\langle P_2\rangle \neq 0$ and $\langle\tau\rangle \neq 0$ (for a nematic phase it would be $\langle P_2\rangle \neq 0$ and $\langle\tau\rangle = 0$). Therefore, these properties allow an unambiguous identification of the phases exhibited.

Table 2. Total Simulation Length (ns) of the Various MD Runs at Temperatures T (K) for Different Model Systems

T/Q	Q0.7	Q0.8	Q0.9	Q1.0[a]	Q1.1	Q1.2
375	100	55	76	121[b]	50	75
400	75	125	105	124	75	75
425	175	125	130	135	75	125
450	300	150	275	135	125	100
475	50	300	300	216	200	300
500	50	50	75	459[c]	200	300
525				265	200	300
550				211	200	300
575				135	200	275
600				131	200	300
625					200	300
650					200	150
675					100	175
700						200
725						250
750						175
775						75

[a]Model system investigated in refs 35, 36, and 38. [b]This point was at T = 385 K. [c]This point was at T = 505 K.

Table 1. Partial Charges of the CG Sites of the Model Systems Investigated

site\Q	Q0.7	Q0.8	Q0.9	Q1.0[a]	Q1.1	Q1.2
A	0.32718	0.37392	0.42066	0.46740	0.51414	0.56088
B	0.17934	0.20496	0.23058	0.25620	0.28182	0.30744
M1	0.11774	0.13456	0.15138	0.16820	0.18502	0.20184
M2	0.04515	0.05160	0.05805	0.06450	0.07095	0.07740
M3	0.02037	0.02328	0.02619	0.02910	0.03201	0.03492
M4	0.01022	0.01168	0.01314	0.01460	0.01606	0.01752
C	0.00000	0.00000	0.00000	0.00000	0.0000	0.00000
E	0.00000	0.00000	0.00000	0.00000	0.0000	0.00000
D	−0.70000	−0.80000	−0.90000	−1.0000	−1.1000	−1.2000

[a]Model system investigated in refs 35, 36, and 38.

DOI: 10.1021/acs.jpcb.6b04717
J. Phys. Chem. B 2016, 120, 9152−9160

In Figure 2 we report the density profile for the system **Q0.8**. The phase at 400 K is very ordered with a clear arrangement of

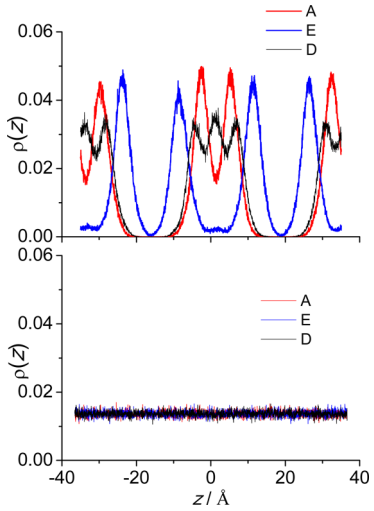

Figure 2. Density modulation, $\rho(z)$, along the director for the system **Q0.8** at (top) 400 K, crystal phase; and (bottom) 500 K, isotropic phase. Traces refer to (red) site A; (black) site D; (blue) site E.

the cations and anions. The ionic layer roughly in the middle of the box shows two peaks of the cation heads (red line), while the anion's profile (black line) has maxima at shifted positions indicating an ordered lattice in the ionic layer. The blue line represents the cation's tail, site E, and it also appears well ordered. The arrangement of the molecules in the crystal phase of the system **Q0.8** is shown in Figure 3.

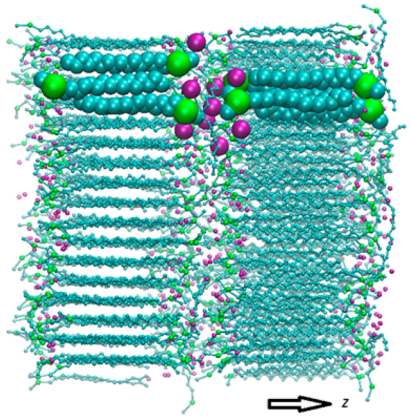

Figure 3. Snapshot of the crystal phase of system **Q0.8** at 400 K with a few selected molecules highlighted, showing the molecular arrangement. The director is aligned along the indicated z-axis.

At the transition point, that is between 475 and 500 K, the system melts and the phase becomes isotropic, as indicated by the constant profile of $\rho(z)$ in the bottom panel of Figure 2. The profiles for the other two systems, **Q0.7** and **Q0.9**, which do not exhibit a smectic phase, are qualitatively similar, at low and high temperature, and they will not be reported here.

In Figure 4 we show the density profiles along the director for the system **Q1.1**. The phase at 400 K (top panel) appears similar to the one observed for the system **Q0.8** at the same temperature, despite the fact that the higher charge makes the peaks sharper and higher in intensity. The phase at 675 K is

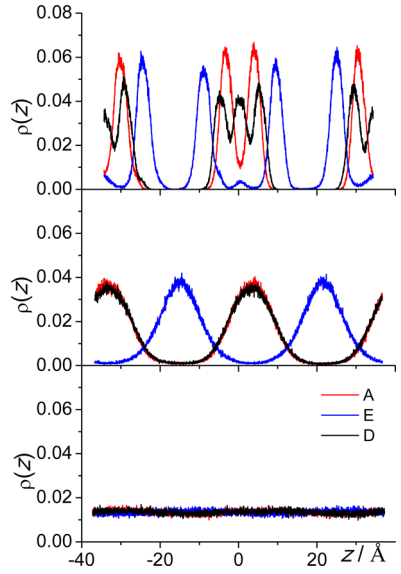

Figure 4. Density modulation, $\rho(z)$, along the director for the system **Q1.1** at (top) 400 K, crystal phase; (middle) 600 K, smectic A phase; and (bottom) 675 K, isotropic phase. Traces refer to (red) site A; (black) site D; (blue) site E.

clearly assigned as the isotropic phase since it lacks any translational order and it has a constant profile of $\rho(z)$. However, for this system, similarly to what is observed for the original **Q1.0** system,[35,36] we find a new phase between the crystal and the isotropic liquid. The density profile at 600 K is strongly modulated but featureless, as expected for a liquid crystal phase of the smectic type. Moreover, the cation head profile and the anion profile are now perfectly overlapped, indicating the lack of translational order within the ionic layer. Consistently, the cation tails, site E, are now preferentially located roughly in the middle of the hydrophobic layer, as expected for a system with molten alkyl chains undergoing several gauche/trans transitions. The arrangement of the molecules in the SmA phase of the system **Q1.1** is shown in Figure 5. A similar sequence of phases is also found for the system **Q1.2**.

3.2. Order Parameters. The orientational order parameter, $\langle P_2 \rangle$, is the ensemble average of the second Legendre polynomial of the angle β between the director of the phase

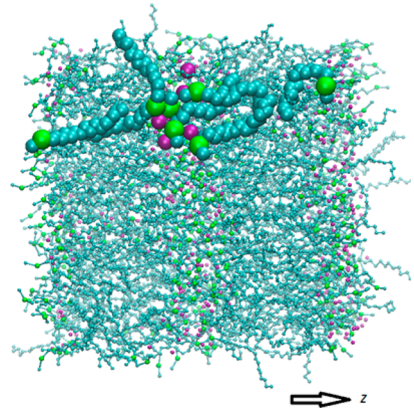

Figure 5. Snapshot of the SmA phase of system **Q1.1** at 600 K with a few selected molecules highlighted, showing the molecular arrangement. The director is aligned along the indicated z-axis.

DOI: 10.1021/acs.jpcb.6b04717
J. Phys. Chem. B 2016, 120, 9152−9160

(here the z-axis) and the vector connecting the head and tail of the cation,

$$\langle P_2 \rangle = \langle P_2(\cos \beta) \rangle \quad (1)$$

Its behavior is shown in Figure 6. We note that for model systems **Q0.7**, **Q0.8**, and **Q0.9**, there is an abrupt drop of the orientational order parameter from a high value, around 0.9, typical of highly ordered phases, to almost zero as expected for isotropic phases (finite box size and simulation length prevent the average value to be exactly zero). As discussed already in refs 35 and 36, a relatively narrow range of the smectic phase is observed for model system **Q1.0** with a low value of the orientational order parameter between 0.1 and 0.25. The orientational order parameter is, instead, significantly higher in the SmA phase of the model systems **Q1.1** and **Q1.2**, reaching values between 0.3 and 0.5.

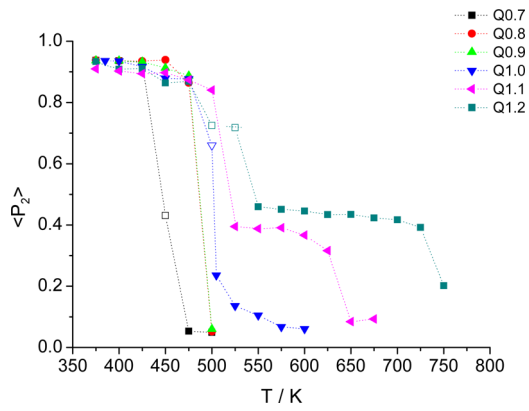

Figure 6. Orientational order parameter values for the model systems with different total charges as a function of temperature. Empty markers correspond to biphasic systems (see text).

The translational order parameter, $\langle \tau_1 \rangle$, is defined as

$$\langle \tau_1 \rangle = |\langle \exp i2\pi z/d \rangle| \quad (2)$$

where z is the position of the molecule along the director and d the smectic periodicity.

The translational order parameter allows us to identify the liquid crystal phase as smectic and to differentiate it from a putative nematic phase where only the orientational order would be present but no density modulation along the director.

In Figure 7 we show the calculated translational order parameters as a function of the temperature for the systems investigated. The values are relatively high (around 0.8) for the crystal phases and decrease close to zero for the isotropic liquid phases. In contrast, they have intermediate values for the three observed smectic phases: between 0.2 and 0.5 for the **Q1.0** system; around 0.7 for the **Q1.1** system; remaining quite high for the **Q1.2** system. This indicates that the translational order of the smectic phase is strongly influenced by the total charge of the ions: a higher charge produces a more defined alternation of ionic/hydrophobic layers, therefore a larger value of the translational order parameter.

Another interesting property that confirms the identification of the phases is the contribution to the total energy coming from the dihedral angles of the alkyl chains. This is shown in Figure 8.

We note that in the Cr phase, all systems exhibit a very similar dihedral energy essentially corresponding to an all-trans configuration for almost all molecules. The energy increases

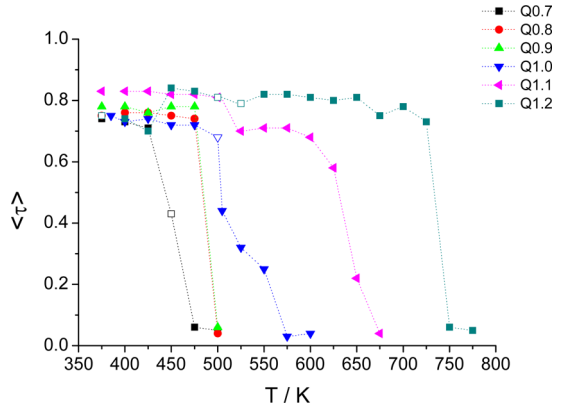

Figure 7. Translational order parameter of the model systems with different total charges as a function of temperature. Empty markers correspond to biphasic systems (see text).

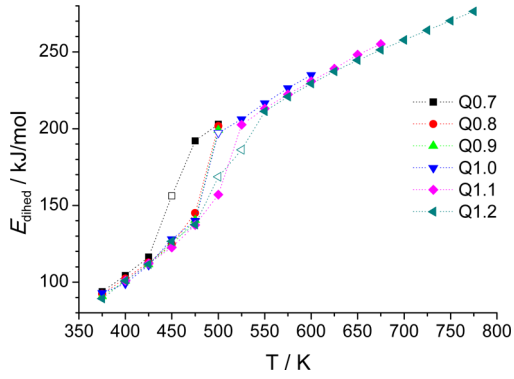

Figure 8. Dihedral energy, E_{dihed}, of the model systems with different total charges as a function of temperature. Empty markers correspond to biphasic systems (see text).

monotonically from about 90 kJ/mol at 375 K up to about 150 kJ/mol at 500 K. As the layers melt, either because of the transition into the isotropic phase (systems **Q0.7**, **Q0.8** and **Q0.9**) or because of the transition into the SmA phase (**Q1.0**, **Q1.1** and **Q1.2**), the dihedral energy jumps to much higher values (ca. 200 kJ/mol) corresponding to an increased conformational freedom of the alkyl chains. The associated ΔE_{dihed} of about 50 kJ/mol is consistent with the enthalpy of melting of long chain alkanes, for example $\Delta H_{melt}(C_{16}H_{34})$ = 51−53 kJ/mol at 291 K.[62] The trends shown in Figure 8 are consistent with the lack of order within the layers of the SmA phase, which is liquid-like, except for the density modulation along the director. Remarkably, there is only a very small jump (hardly visible in Figure 8) in the dihedral energy once the SmA phase clears into the isotropic phase, consistent with the nature of the SmA-Iso transition that involves mostly the loss of the layered structure of the systems (typical ΔH for the SmA-Iso transitions are of the order of one kJ/mol or less).

3.3. Phase Diagram. Having established the type of phase, we now turn our attention to the phase diagram. The transition temperature between phase 1 and phase 2 was estimated as the midpoint between the highest temperature of the low-temperature phase 1 and the lowest temperature of the high-temperature phase 2. In some cases, at a given temperature, we noticed the presence of a two-phase system, with one layer in the low-temperature phase and the other in the high-temperature phase. This occurred for model **Q0.7** at T = 450 K; for model **Q1.0** at T = 500 K and for mode **Q1.2** at T = 500

DOI: 10.1021/acs.jpcb.6b04717
J. Phys. Chem. B 2016, 120, 9152−9160

and 525 K. In these cases, the temperature of the biphasic box was taken as the transition temperature. Error bars are estimated from the step in temperature of the heating run, that is ±25 K.

In Figure 9 we show the phase diagram obtained from the simulation for the model compound under investigation (which

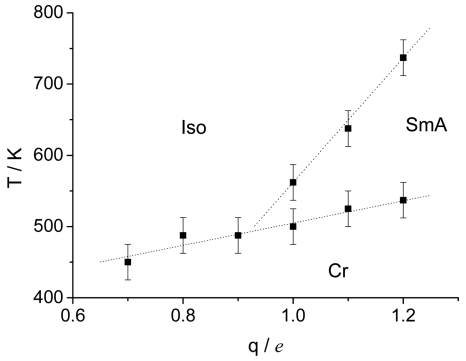

Figure 9. Phase diagram of the CG model system as a function of temperature and total charge.

can be, however, taken as a representative of a generic IL composed of a cation with a charged head and a long alkyl chain paired with a small anion) as a function of the temperature T and total charge Q of the system. We note that by increasing Q from 0.7 up to 1.2 the melting temperature of the crystal phase (that is the transition temperature from the crystal phase into the isotropic liquid or smectic liquid crystal phase) is increased even though the effect is not particularly large. Within the error bars, the effect appears linear with the total charge of the ions. More interesting is the observation that, for a total charge lower than about 0.9, the ionic smectic phase is absent. This is qualitatively in agreement with the expectation of no liquid crystal phase for a nonionic fully flexible system. In fact we note that, based on simple intuitive understanding, we expect the LC phase to be stabilized either by the presence of a so-called mesogenic core, a rigid elongated unit such as cyanobiphenyl, or by microphase segregation of ionic and hydrophobic parts in amphiphilic non/rigid molecules. By reducing the amphiphilic nature of a flexible molecule none of the requirements for a stable LC phase is satisfied. An ionic liquid crystal phase can only be observed for a total charge higher than 0.9. Moreover, its thermal range of stability is very sensitive to the total charge: the clearing point (that is the transition temperature from the smectic phase into the isotropic liquid) strongly increases as the total charge grows to 1.2 times the reference CG model. This qualitatively confirms the strong effect, in the stabilization of ionic liquid crystal phases, coming from the microsegregation between ionic and hydrophobic parts.[38] The increase of the total charge also results in a better agreement with the experimental thermal range for the stability of the SmA phase (although the transition temperatures are still not reproduced quantitatively): in fact the real system exhibits a SmA phase from ca. 325 to 456 K (with some hysteresis between heating and cooling[63]) for a total range of smectic phase of ca. 130 K, which is better reproduced by the model system **Q1.1**.

3.4. Connection between Smectic Layering and Nanosegregation in the Isotropic Phase. It is also of interest to inspect the detailed structures in the isotropic phase obtained for the various systems with different charges. All systems in the isotropic phase are characterized by the same values of the key macroscopic parameters, that is the orientational and translational order parameters, which are close to zero (as much as it is allowed by the finite box size and simulation length) and the distribution function $\rho(z)$ that has a constant profile.

Nevertheless, it is well-known that the isotropic structure of ionic liquids is strongly inhomogeneous at the nanoscopic level. For example, for 1-alkyl-3-methylimidazolium salts, there is evidence of nanosegregation of hydrophobic chains from the polar network of ions, from both computer simulations and scattering experiments, already with butyl chains. The effect increases with the chain length and has been connected to the appearance of smectic phases, as already discussed in the Introduction. Moreover, recent experimental findings have directly related the emergence of the SmA phase in long-chain imidazolium salts to the nanosegregation effect.[64,65] Although macroscopic parameters all give the same picture of an isotropic phase, the heterogeneity order parameter $\langle h \rangle$ introduced by Voth and Wang[44,66] has been developed exactly with the purpose to highlight the level of nanosegregation of a given molecular site in a liquid phase. Its definition is given in eq 3, where r_{ij} is the distance, corrected for periodic boundary conditions, between two identical sites on different molecules, while σ is a scale length parameter given by $(1/\rho)^{1/3}$, with ρ being the density of sites under consideration.

$$\langle h \rangle = \frac{1}{N} \sum_i \sum_j \exp\left(-\frac{r_{ij}^2}{2\sigma^2}\right) \tag{3}$$

In Figure 10 we show the calculated $\langle h \rangle$ obtained in the isotropic phases of the studied systems. The temperatures are

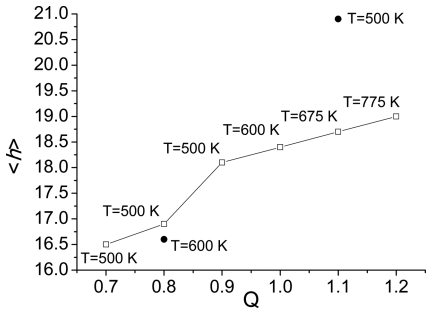

Figure 10. (Empty squares) Heterogeneity order parameter, $\langle h \rangle$ in the isotropic phases of the systems investigated. (Filled circles) Selected systems after a sudden cooling or heating (see text).

obviously different since the clearing point depends on the charge, as we have seen above. However, although the absolute temperatures are different, the "scaled" temperatures defined as $T/T_{m/c}$, where $T_{m/c}$ are either the melting or clearing points, are all very close and comparable. As we can see in Figure 10, the $\langle h \rangle$ values separate the systems into two groups: the low Q systems, namely **Q0.7** and **Q0.8**, and the high Q systems, namely **Q0.9**, **Q1.0**, **Q1.1**, and **Q1.2**. As we move from low to high Qs, we observe a sort of "transition", a finite jump in the $\langle h \rangle$ values, between Q values of 0.8−0.9, indicating a different structure of the isotropic phases of the two subsystems. This observation can be explained as a result of the decreased total charge of the systems and agrees with the finding of two different regimes in the isotropic phase of ILs as a function of temperature:[44] a nanosegregated structure at relatively low

DOI: 10.1021/acs.jpcb.6b04717
J. Phys. Chem. B 2016, 120, 9152−9160

temperature and a homogeneous system at high temperature. The reason for the "transition" shown in Figure 10 is not simply because of the different temperatures: in fact, at higher temperatures, a lower $\langle h \rangle$ value would be expected because of the increased thermal motions. This issue has been confirmed by suddenly heating up the system **Q0.8** from 500 to 600 K and by cooling down the system **Q1.1** from 675 to 500 K and running the simulation for just 2.5 ns (so to avoid possible phase transitions and keep the **Q1.1** system isotropic). The $\langle h \rangle$ parameter calculated over the last 1.25 ns of such simulation is also shown in Figure 10 (filled circles), which clearly shows that the effect of the temperature is as expected: slightly lower for **Q0.8**, which is already in the homogeneous isotropic phase; very significant in the **Q1.1** system which, by cooling, nanosegregates much more. Therefore, the observed jump in $\langle h \rangle$ of the isotropic phase as a function of the total charge is truly and only related to the different total charges that enhance or quench the nanosegregation of the isotropic phase.

Remarkably the "transition" from a more homogeneous to a more nanosegregated isotropic liquid phase is almost perfectly overlapped with the emergence of a SmA phase in the phase diagram. Therefore, we can establish a direct link between the nanosegregation in the isotropic phase of ILs and the stability of an ionic smectic mesophase.

4. CONCLUSIONS

We have investigated the effect of the total charge of cation and anion on the phase behavior of a model imidazolium ionic liquid crystal. The results of the simulations clearly indicate that the microphase segregation, which is responsible for the existence of ionic smectic phases, is strongly increased by the total charge of the ions. For charges lower than about 0.9*e*, the ionic smectic phase is absent, and the crystal directly melts into an isotropic phase. For the systems with a larger charge, the thermal range of stability of the ionic smectic phase is significantly increased, mostly as a result of a higher clearing point into the isotropic liquid. By contrast, the melting of the crystal phase is much less affected. These results consistently indicate that the ILC phase is stabilized by microphase segregation between the hydrophobic layers and the ionic layers. We have also analyzed the structure of the ionic liquid phase for the models with different charges and observed the same transition from a homogeneous to a nanosegregated structure already reported by Wang and Voth for ionic liquids as a function of temperature.[44]

If we combine these observations with the results of our recent work,[38] where it was shown that the smectic phase has a higher degree of nanosegregation, as measured by the $\langle h \rangle$ parameter, than the isotropic phase at the same temperature, then the following picture from the viewpoint of thermodynamics emerges. Both the increase of the alkyl chain length and the increase of the total charge of the cation head and anion do intensify the competition between hydrophobic and electrostatic interactions. Such competition leads to microphase segregation between the alkyl chains and the ionic network of ions, and such segregation is higher in the smectic phase compared to the isotropic phase. Therefore, ionic smectic phases are stabilized either by increasing the length of the alkyl chain, as well-documented in the literature, and/or by increasing the total charge in the ionic parts as we have shown here. In all cases the enthalpy loss due to the mixing of these two parts of the molecules cannot be easily compensated by the entropy gain due to the increased disorder, unless one reaches higher and higher temperatures.

AUTHOR INFORMATION

Corresponding Author

*E-mail: giacomo.saielli@unipd.it.

Author Contributions

The manuscript was written through contributions of all authors. All authors have given approval to the final version of the manuscript.

Notes

The authors declare no competing financial interest.

ACKNOWLEDGMENTS

This work was sponsored by CNR (National Research Council, Italy) and CAS (Chinese Academy of Sciences, China) through a CNR-CAS bilateral agreement 2014-2016. Computer time was granted by CINECA (ISCRA project HP10BZQZGE), and the Laboratorio Interdipartimentale di Chimica Computazionale (LICC) of the University of Padova. Financial support from MIUR (PRIN HI-PHUTURE 2010N3T9M4_001, FIRB RBAP11C58Y_003 "'NanoSolar'") and Fondazione CARIPARO "Nano-Mode - Progetti di Eccellenza 2010" and from the National Natural Science Foundation of China (Nos. 11274319 and 11421063) is also gratefully acknowledged.

ABBREVIATIONS

IL:ionic liquid; ILC:ionic liquid crystal; LC:liquid crystal; MD:molecular dynamics; RDF:radial distribution function; CGFF:coarse-grained force field; FAFF:fully atomistic force field; HOP:heterogeneity order parameter

REFERENCES

(1) Binnemans, K. Ionic Liquid Crystals. *Chem. Rev.* **2005**, *105*, 4148−4204.

(2) Axenov, K. V.; Laschat, S. Thermotropic Ionic Liquid Crystals. *Materials* **2011**, *4*, 206−259.

(3) Causin, V.; Saielli, G. Ionic Liquid Crystals. In *Green Solvents II. Properties and Applications of Ionic Liquids*; Mohammad, A., Inamuddin, D., Eds.; Springer: Dordrecht, The Netherlands, 2012; pp 79−118.

(4) Goossens, K.; Lava, K.; Bielawski, C. W.; Binnemans, K. Ionic Liquid Crystals: Versatile Materials. *Chem. Rev.* **2016**, *116*, 4643−4807.

(5) Bowlas, C. J.; Bruce, D. W.; Seddon, K. R. Liquid-Crystalline Ionic Liquids. *Chem. Commun.* **1996**, 1625−1626.

(6) Holbrey, J. D.; Seddon, K. R. The Phase Behaviour of 1-Alkyl-3-Methylimidazolium Tetrafluoroborates; Ionic Liquids and Ionic Liquid Crystals. *J. Chem. Soc., Dalton Trans.* **1999**, 2133−2140.

(7) Binnemans, K.; Van Deun, R.; Thijs, B.; Vanwelkenhuysen, I.; Geuens, I. Structure and Mesomorphism of Silver Alkanoates. *Chem. Mater.* **2004**, *16*, 2021−2027.

(8) Casella, G.; Causin, V.; Rastrelli, F.; Saielli, G. Viologen-Based Ionic Liquid Crystals: Induction of a Smectic A Phase by Dimerisation. *Phys. Chem. Chem. Phys.* **2014**, *16*, 5048−5051.

(9) Klimusheva, G.; Mirnaya, T.; Garbovskiy, Y. Versatile Nonlinear-Optical Materials Based on Mesomorphic Metal Alkanoates: Design, Properties, and Applications. *Liq. Cryst. Rev.* **2015**, *3*, 28−57.

(10) Yamanaka, N.; Kawano, R.; Kubo, W.; Masaki, N.; Kitamura, T.; Wada, Y.; Watanabe, M.; Yanagida, S. Dye-Sensitized TiO2 Solar Cells using Imidazolium-Type Ionic Liquid Crystal Systems as Effective Electrolytes. *J. Phys. Chem. B* **2007**, *111*, 4763−4769.

(11) Yamanaka, N.; Kawano, R.; Kubo, W.; Kitamura, T.; Wada, Y.; Watanabe, M.; Yanagida, S. Ionic Liquid Crystal as a Hole Transport Layer of Dye-Sensitized Solar Cells. *Chem. Commun.* **2005**, 740−742.

DOI: 10.1021/acs.jpcb.6b04717
J. Phys. Chem. B 2016, 120, 9152−9160

(12) Henmi, M.; Nakatsuji, K.; Ichikawa, T.; Tomioka, H.; Sakamoto, T.; Yoshio, M.; Kato, T. Self-Organized Liquid-Crystalline Nanostructured Membranes for Water Treatment: Selective Permeation of Ions. *Adv. Mater.* **2012**, *24*, 2238−2241.
(13) Yoshio, M.; Kagata, T.; Hoshino, K.; Mukai, T.; Ohno, H.; Kato, T. One-Dimensional Ion-Conductive Polymer Films: Alignment and Fixation of Ionic Channels Formed by Self-Organization of Polymerizable Columnar Liquid Crystals. *J. Am. Chem. Soc.* **2006**, *128*, 5570−5577.
(14) Safavi, A.; Tohidi, M. Design and Characterization of Liquid Crystal-Graphite Composite Electrodes. *J. Phys. Chem. C* **2010**, *114*, 6132−6140.
(15) Shvedene, N. V.; Avramenko, O. A.; Baulin, V. E.; Tomilova, L. G.; Pletnev, I. V. Iodide-Selective Screen-Printed Electrodes Based on Low-Melting Ionic Solids and Metallated Phthalocyanine. *Electroanalysis* **2011**, *23*, 1067−1072.
(16) Beneduci, A.; Cospito, S.; La Deda, M.; Veltri, L.; Chidichimo, G. Electrofluorochromism in Pi-Conjugated Ionic Liquid Crystals. *Nat. Commun.* **2014**, *5*, 3105.
(17) Cospito, S.; Beneduci, A.; Veltri, L.; Salamonczyk, M.; Chidichimo, G. Mesomorphism and Electrochemistry of Thienoviologen Liquid Crystals. *Phys. Chem. Chem. Phys.* **2015**, *17*, 17670−17678.
(18) Uchida, Y.; Matsumoto, T.; Akita, T.; Nishiyama, N. Ion Conductive Properties in Ionic Liquid Crystalline Phases Confined in a Porous Membrane. *J. Mater. Chem. C* **2015**, *3*, 6144−6147.
(19) Bedrov, D.; Borodin, O. Thermodynamic, Dynamic, and Structural Properties of Ionic Liquids Comprised of 1-Butyl-3-Methylimidazolium Cation and Nitrate, Azide, Or Dicyanamide Anions. *J. Phys. Chem. B* **2010**, *114*, 12802−12810.
(20) Bedrov, D.; Borodin, O.; Li, Z.; Smith, G. D. Influence of Polarization on Structural, Thermodynamic, and Dynamic Properties of Ionic Liquids obtained from Molecular Dynamics Simulations. *J. Phys. Chem. B* **2010**, *114*, 4984−4997.
(21) Borodin, O. Polarizable Force Field Development and Molecular Dynamics Simulations of Ionic Liquids. *J. Phys. Chem. B* **2009**, *113*, 11463−11478.
(22) Borodin, O.; Gorecki, W.; Smith, G. D.; Armand, M. Molecular Dynamics Simulation and Pulsed-Field Gradient NMR Studies of Bis(Fluorosulfonyl)Imide (FSI) and Bis[(Trifluoromethyl)Sulfonyl]-Imide (TFSI)-Based Ionic Liquids. *J. Phys. Chem. B* **2010**, *114*, 6786−6798.
(23) Smith, G. D.; Borodin, O.; Magda, J. J.; Boyd, R. H.; Wang, Y.; Bara, J. E.; Miller, S.; Gin, D. L.; Noble, R. D. A Comparison of Fluoroalkyl-Derivatized Imidazolium:TFSI and Alkyl-Derivatized Imidazolium:TFSI Ionic Liquids: A Molecular Dynamics Simulation Study. *Phys. Chem. Chem. Phys.* **2010**, *12*, 7064−7076.
(24) Canongia Lopes, J. N.; Padua, A. A. H. Molecular Force Field for Ionic Liquids III: Imidazolium, Pyridinium, and Phosphonium Cations; Chloride, Bromide, and Dicyanamide Anions. *J. Phys. Chem. B* **2006**, *110*, 19586−19592.
(25) Canongia Lopes, J. N.; Padua, A. A. H.; Shimizu, K. Molecular Force Field for Ionic Liquids IV: Trialkylimidazolium and Alkoxycarbonyl-Imidazolium Cations; Alkylsulfonate and Alkylsulfate Anions. *J. Phys. Chem. B* **2008**, *112*, 5039−5046.
(26) Migliorati, V.; Serva, A.; Aquilanti, G.; Pascarelli, S.; D'Angelo, P. Local Order and Long Range Correlations in Imidazolium Halide Ionic Liquids: A Combined Molecular Dynamics and XAS Study. *Phys. Chem. Chem. Phys.* **2015**, *17*, 16443−16453.
(27) Migliorati, V.; Serva, A.; Aquilanti, G.; Olivi, L.; Pascarelli, S.; Mathon, O.; D'Angelo, P. Combining EXAFS Spectroscopy and Molecular Dynamics Simulations to Understand the Structural and Dynamic Properties of an Imidazolium Iodide Ionic Liquid. *Phys. Chem. Chem. Phys.* **2015**, *17*, 2464−2474.
(28) Migliorati, V.; Zitolo, A.; D'Angelo, P. Using a Combined Theoretical and Experimental Approach to Understand the Structure and Dynamics of Imidazolium-Based Ionic Liquids/Water Mixtures. 1. MD Simulations. *J. Phys. Chem. B* **2013**, *117*, 12505−12515.
(29) Saielli, G. Fully-Atomistic Simulations of the Ionic Liquid Crystal $[C_{16}MIm][NO_3]$: Orientational Order Parameters and Voids Distribution. *J. Phys. Chem. B* **2016**, *120*, 2569−2577.
(30) Frezzato, D.; Saielli, G. Distribution and Dynamic Properties of Xenon Dissolved in the Ionic Smectic Phase of $[C_{16}mim][NO_3]$: MD Simulation and Theoretical Model. *J. Phys. Chem. B* **2016**, *120*, 2578−2585.
(31) Berardi, R.; Muccioli, L.; Zannoni, C. Can Nematic Transitions be Predicted by Atomistic Simulations? A Computational Study of the Odd Even Effect. *ChemPhysChem* **2004**, *5*, 104−111.
(32) Pizzirusso, A.; Savini, M.; Muccioli, L.; Zannoni, C. An Atomistic Simulation of the Liquid-Crystalline Phases of Sexithiophene. *J. Mater. Chem.* **2011**, *21*, 125−133.
(33) Cacelli, I.; Prampolini, G.; Tani, A. Atomistic Simulation of a Nematogen using a Force Field Derived from Quantum Chemical Calculations. *J. Phys. Chem. B* **2005**, *109*, 3531−3538.
(34) Boyd, N. J.; Wilson, M. R. Optimization of the GAFF Force Field to Describe Liquid Crystal Molecules: The Path to a Dramatic Improvement in Transition Temperature Predictions. *Phys. Chem. Chem. Phys.* **2015**, *17*, 24851−24865.
(35) Saielli, G. MD Simulation of the Mesomorphic Behaviour of 1-Hexadecyl-3-Methylimidazolium Nitrate: Assessment of the Performance of a Coarse-Grained Force Field. *Soft Matter* **2012**, *8*, 10279−10287.
(36) Saielli, G.; Voth, G. A.; Wang, Y. Diffusion Mechanisms in Smectic Ionic Liquid Crystals: Insights from Coarse-Grained MD Simulations. *Soft Matter* **2013**, *9*, 5716−5725.
(37) Ji, Y.; Shi, R.; Wang, Y.; Saielli, G. Effect of the Chain Length on the Structure of Ionic Liquids: From Spatial Heterogeneity to Ionic Liquid Crystals. *J. Phys. Chem. B* **2013**, *117*, 1104−1109.
(38) Saielli, G.; Bagno, A.; Wang, Y. Insights on the Isotropic-to-Smectic A Transition in Ionic Liquid Crystals from Coarse-Grained Molecular Dynamics Simulations: The Role of Microphase Segregation. *J. Phys. Chem. B* **2015**, *119*, 3829−3836.
(39) Urahata, S. M.; Ribeiro, M. C. C. Structure of Ionic Liquids of 1-Alkyl-3-Methylimidazolium Cations: A Systematic Computer Simulation Study. *J. Chem. Phys.* **2004**, *120*, 1855−1863.
(40) Wang, Y.; Voth, G. A. Unique Spatial Heterogeneity in Ionic Liquids. *J. Am. Chem. Soc.* **2005**, *127*, 12192−12193.
(41) Canongia Lopes, J. N. A.; Pàdua, A. A. H. Nanostructural Organization in Ionic Liquids. *J. Phys. Chem. B* **2006**, *110*, 3330−3335.
(42) Triolo, A.; Russina, O.; Bleif, H.; Di Cola, E. Nanoscale Segregation in Room Temperature Ionic Liquids. *J. Phys. Chem. B* **2007**, *111*, 4641−4644.
(43) Zhao, H. -Q.; Shi, R.; Wang, Y. Nanoscale Tail Aggregation in Ionic Liquids: Roles of Electrostatic and Van Der Waals Interactions. *Commun. Theor. Phys.* **2011**, *56*, 499−503.
(44) Wang, Y.; Voth, G. A. Tail Aggregation and Domain Diffusion in Ionic Liquids. *J. Phys. Chem. B* **2006**, *110*, 18601−18608.
(45) Dommert, F.; Wendler, K.; Berger, R.; Delle Site, L.; Holm, C. Force Fields for Studying the Structure and Dynamics of Ionic Liquids: A Critical Review of Recent Developments. *ChemPhysChem* **2012**, *13*, 1625−1637.
(46) Holloczki, O.; Malberg, F.; Welton, T.; Kirchner, B. On the Origin of Ionicity in Ionic Liquids. Ion Pairing Versus Charge Transfer. *Phys. Chem. Chem. Phys.* **2014**, *16*, 16880−16890.
(47) Matsumiya, M.; Hata, K.; Tsunashima, K. Self-Diffusion Behaviors of Ionic Liquids by MD Simulation Based on United-Atom Force Field Introduced Charge Scaling by Ab Initio MO Simulation. *J. Mol. Liq.* **2015**, *203*, 125−130.
(48) Shimizu, J.; Imamura, K.; Nogami, T.; Mikawa, H. Phase Transition of Quaternary Alkyl Halide Salts of 1,4-Diazabicyclo2.2.2]-Octane. *Bull. Chem. Soc. Jpn.* **1986**, *59*, 1443−1448.
(49) Ohta, K.; Sugiyama, T.; Nogami, T. A Smectic T Phase of 1,4-Dialkyl-1,4-diazoniabicyclo2.2.2]Octane Dibromides. *J. Mater. Chem.* **2000**, *10*, 613−616.
(50) Bhowmik, P. K.; Han, H. S.; Nedeltchev, I. K.; Cebe, J. J. Room-Temperature Thermotropic Ionic Liquid Crystals: Viologenbis-(Triflimide) Salts. *Mol. Cryst. Liq. Cryst.* **2004**, *419*, 27−46.

DOI: 10.1021/acs.jpcb.6b04717
J. Phys. Chem. B 2016, 120, 9152−9160

(51) Causin, V.; Saielli, G. Effect of Asymmetric Substitution on the Mesomorphic Behaviour of Low-Melting Viologen Salts of Bis-(Trifluoromethanesulfonyl)Amide. *J. Mater. Chem.* **2009**, *19*, 9153−9162.
(52) Casella, G.; Causin, V.; Rastrelli, F.; Saielli, G. Ionic Liquid Crystals Based on Viologen Dimers: Tuning the Mesomorphism by Varying the Conformational Freedom of the Ionic Layer. *Liq. Cryst.* **2016**, *43*, 1161−1173.
(53) Bonchio, M.; Carraro, M.; Casella, G.; Causin, V.; Rastrelli, F.; Saielli, G. Thermal Behaviour and Electrochemical Properties of Bis(Trifluoromethanesulfonyl)Amide and Dodecatungstosilicate Viologen Dimers. *Phys. Chem. Chem. Phys.* **2012**, *14*, 2710−2717.
(54) Zhou, N.; Zhao, G.; Dong, K.; Sun, J.; Shao, H. Investigations on a Series of Novel Ionic Liquids Containing the Closo-B12Cl12]2-Dianion. *RSC Adv.* **2012**, *2*, 9830−9838.
(55) Palgunadi, J.; Kwon, O.; Lee, H.; Bae, J. Y.; Ahn, B. S.; Min, N.; Kim, H. S. Ionic Liquid-Derived Zinc Tetrahalide Complexes: Structure and Application to the Coupling Reactions of Alkylene Oxides and CO2. *Catal. Today* **2004**, *98*, 511−514.
(56) Deschenaux, R.; Schweissguth, M.; Levelut, A. Electron-Transfer Induced Mesomorphism in the Ferrocene-Ferrocenium Redox System: First Ferrocenium-Containing Thermotropic Liquid Crystal. *Chem. Commun.* **1996**, 1275−1276.
(57) Jankowiak, A.; Sivaramamoorthy, A.; Pociecha, D.; Kaszynski, P. How Much do Coulombic Interactions Stabilize a Mesophase? Ion Pair and Non-Ionic Binary Isosteric Derivatives of Monocarbaborates and Carboranes. *RSC Adv.* **2014**, *4*, 53907−53914.
(58) Piechocki, C.; Simon, J.; André, J.; Guillon, D.; Petit, P.; Skoulios, A.; Weber, P. Synthesis and Physico-Chemical Studies of Neutral and Chemically Oxidized Forms of Bis-(Octaalkyloxyphthalocyaninato) Lutetium. *Chem. Phys. Lett.* **1985**, *122*, 124−128.
(59) Wang, Y.; Feng, S.; Voth, G. A. Transferable Coarse-Grained Models for Ionic Liquids. *J. Chem. Theory Comput.* **2009**, *5*, 1091−1098.
(60) Wang, Y.; Noid, W. G.; Liu, P.; Voth, G. A. Effective Force Coarse-Graining. *Phys. Chem. Chem. Phys.* **2009**, *11*, 2002−2015.
(61) Smith, W.; Forester, T. R.; Todorov, I. T. DL_POLY Classic. www.ccp5.ac.uk/DL_POLY_CLASSIC, 2010 (Last accessed August 1st, 2016).
(62) Acree, W. E.; Chickos, J. S., Eds. Phase Transition Enthalpy Measurements of Organic and Organometallic Compounds. In *NIST Chemistry WebBook, NIST Standard Reference Database Number 69*; Linstrom, P. J., Mallard, W. G., Eds.; January 8, 2015.
(63) Guillet, E.; Imbert, D.; Scopelliti, R.; Bunzli, J. G. Tuning the Emission Color of Europium-Containing Ionic Liquid-Crystalline Phases. *Chem. Mater.* **2004**, *16*, 4063−4070.
(64) Nemoto, F.; Kofu, M.; Yamamuro, O. Thermal and Structural Studies of Imidazolium-Based Ionic Liquids with and without Liquid-Crystalline Phases: The Origin of Nanostructure. *J. Phys. Chem. B* **2015**, *119*, 5028−5034.
(65) Kofu, M.; Tyagi, M.; Inamura, Y.; Miyazaki, K.; Yamamuro, O. Quasielastic Neutron Scattering Studies on Glass-Forming Ionic Liquids with Imidazolium Cations. *J. Chem. Phys.* **2015**, *143*, 234502.
(66) Wang, Y.; Voth, G. A. Molecular Dynamics Simulations of Polyglutamine Aggregation using Solvent-Free Multiscale Coarse-Grained Models. *J. Phys. Chem. B* **2010**, *114*, 8735−8743.

DOI: 10.1021/acs.jpcb.6b04717
J. Phys. Chem. B 2016, 120, 9152−9160